Early pathogenic events during the vascular calcification of uremic rats

Luis Hortells[1] DVM, PhD; Cecilia Sosa[1] DVM, PhD; Ángel Millán[2] MS Chem, PhD; Víctor Sorribas[1]* DVM, PhD.

[1]Laboratory of Molecular Toxicology, University of Zaragoza. [2]Institute of Materials Science, University of Zaragoza.

*Corresponding author:

Prof. Víctor Sorribas

University of Zaragoza, Veterinary Faculty, Department of Toxicology

Calle Miguel Servet 177

E50013 Zaragoza, Spain.

Fax: +34 976761612

Phone: +34976761631

sorribas@unizar.es

Sources of support: Grants SAF2012-33898 and SAF2015-66705-P to V.S. and MAT2014-54975-R to AM, all three from the Spanish MINECO/FEDER.

Running title: Early Pathogenesis of Vascular Calcification

Abstract

Vascular calcification (VC) in chronic kidney disease is a very complex process that has been traditionally explained in multifactorial terms. In this work we have aimed to clarify the relevance of the diverse agents acting on VC in uremic rats and distinguish between initiating and complicating factors. 5/6 Nephrectomized rats fed a 1.2% Pi diet were analyzed at different time points. The earliest changes observed in the aortic wall were noticed 11 weeks after nephrectomy: increased Dickkopf-related protein 1 (Dkk1) mRNA expression and tissue non-specific alkaline phosphatase (TNAP) expression and activity. First deposits of aortic Ca^{2+} were observed after 12 weeks in areas of TNAP expression. Increased mRNA expressions of Runx2, BMP2, Pit1, Pit2, HOXA10, PHOSPHO1, Fetuin-A, ANKH, OPN, Klotho, and ENPP1 were also found after TNAP changes. Increased concentrations of activin A and FGF23 in plasma were observed as from the first moments of nephrectomy, while PTH and hyperphosphatemia only increased after 20 weeks. Neither blood nor aortic PPi were modified, nor the aortic expression of matrix Gla protein, Msx2, several carbonic anhydrases, osteoprotegerin, PTH receptor-1, annexins II and V, and CD39. In conclusion, increased TNAP and Dkk1 expression in aorta precedes initial calcium deposition, which is only preceded by changes in blood renal parameters. Other calcification agents are only expressed at later stages, in a complex branching pattern that needs to be understood.

Key words: Vascular calcification, pathogenesis, uremia, early events, TNAP, Dkk1

Introduction

The ectopic calcification of large arteries is a common complication in chronic kidney disease (CKD), and in combination with abnormalities in circulating biomarkers and bone histomorphometry, it forms a part of CKD-mineral bone disorder (CKD-MBD).[1] Cardiovascular complications are the main cause of mortality in CKD patients, and medial vascular calcification (VC) is a contributing factor through arterial stiffening, left ventricle overload and hypertrophy, increased pulsatility, inappropriate blood supply to the organs, insufficient force for venous return, etc.[2]

Calcium phosphate deposition in large arteries ends in the form of hydroxyapatite deposits, which cause structural changes to the wall layers, accompanied by gene expression and phenotype modifications of the vascular smooth muscle cells (VSMC) towards a pro-calcific, osteochondrogenic phenotype.[3] Among the bone-forming genes, these cells overexpress phosphatases such as tissue non-specific alkaline phosphatase[4] (TNAP) and PHOSPHO1,[5] which, among other activities, hydrolyze the calcification inhibitor, pyrophosphate (PPi). Many other mechanisms have been proposed as mediators of the calcification of VSMC: the formation of matrix vesicles, apoptotic bodies,[6] and exosomes[7] that serve as nucleation sites for heterogeneous calcium phosphate precipitation, the overexpression of Pi transporters,[8] an altered extracellular matrix, enzymatic elastin degradation,[9] etc. In addition, during the formation of CKD-MBD, hormonal network disorders such as the increased secretion of fibroblast growth factor 23 (FGF23) and a decreased abundance of soluble Klotho also seem to be involved in VC pathogenesis.[10] More recently, the deleterious effects on the vasculature caused by circulating Wnt inhibitors produced by an injured kidney have been described. Such effects could include dedifferentiation of VSMC towards osteoblastic transition and vascular calcification,[11] as well as endothelial-to-mesenchymal transition in the vasculature of CKD and atherogenic animal models.[12] Finally, the use of a ligand trap in an $ldlr^{-/-}$ mouse with ablative CKD has shown that another repair factor, activin A, is released from an injured kidney into the

systemic circulation and is involved in the dedifferentiation of VSMC, in osteoblastic transition, and in neointimal plaque calcification.[13]

In this work, we attempt to clarify some aspects of this puzzling and complex pathogenic scenario of vascular dysfunction and ectopic calcification during CKD. In the search for a less complex model, the *in vitro* methods of Pi-induced calcification were discarded.[14] Therefore, for the sake of simplicity we have studied the very early stages of aortic calcification during CKD using the 5/6-nephrectomized (NX) rat model, in which rats were fed a Pi-rich diet. The aorta calcium content, the specific gene expression changes, serum and urine parameters, and protein expression and activities were analyzed at different times as from nephrectomy. Our findings have allowed us to discriminate between the initiating and the complicating pathogenic events of VC and to identify the changes that occur before the first calcium deposits are observed by electron microscopy.

Results

Blood plasma analysis. One week after the 5/6NX, animals were given free access to a 1.2% Pi diet and water. Fig. 1 shows the experimental design, the times of sacrifice, and the main hits of our work in the aorta. Table 1 shows some plasma biochemical parameters at each time point. As expected, in the 5/6NX animals (a model of stages 3-4 CKD), the urea and creatinine concentrations had increased at all analyzed times. Calcium was not modified, and despite the nephrectomy and despite the fact that the animals were eating food with Pi that was twice the control concentration, the plasma Pi only increased at week 20, when the PTH also increased. The low concentration of Pi at earlier times was most likely maintained by both the mechanism of renal and intestinal adaptation to a high Pi diet and by the phosphatonin FGF23, which was 13.5 times higher at week 11 and 22 times higher at week 12 compared to the control rats. Interestingly, the concentrations of neither the VC inhibitor PPi, the cytokine TNFα, the circulating Klotho, nor the Wnt inhibitor Dkk1 were altered in the plasma, even after 20 weeks. Activin A, however, was statistically increased at all four time points.

Aorta calcification. Aorta calcification was studied in several ways. First, the traditional stainings of calcium using alizarin red and of phosphate using von Kossa were only positive after 20 weeks (Fig. 2A for weeks 12 and 20). The positive picture after 20 weeks is an example of intense calcification, but the variability of staining was very high, with some areas and sections negative from the same animals. To confirm these findings, the calcium content was colorimetrically quantified, and based on the higher sensitivity of colorimetry over histological staining, the results showed a significant increase of calcium in the aorta already at 12 weeks after nephrectomy (Fig. 2B). This finding was corroborated in a confirmatory experiment that also included nephrectomized animals eating 0.6% Pi-containing food and sham-operated animals that ate 0.6% and 1.2% Pi for the same period of time (Fig. 2B, inset). Only the nephrectomized animals eating the 1.2% Pi diet showed a calcium content increase at week 12.

To clarify these divergent results between calcium staining and colorimetric determination, aorta sections were studied by electron microscopy. At week 11, no calcium deposits were observed by SEM analysis. However, the first calcium deposits of less than a micron were observed after 12 weeks (Fig. 2C). Field emission SEM revealed that there were two types of deposits from the 12-week nephrectomized animals according to the Ca/P ratios (Fig. 2D): the most frequent deposits had a ratio of 1.35, compatible with amorphous calcium phosphate, while a few of the deposits had a ratio of 1.65, compatible with hydroxyapatite (i.e., a more crystalline form of calcium phosphate). The analyses of the aortas from sham-operated rats eating a 1.2% Pi diet and from 5/6NX rats eating a 0.6% Pi diet were negative for the presence of calcium deposits.

Gene expression analysis: Genes likely to be involved in vascular calcification were analyzed using quantitative, real-time PCR. The genes that were not modified even 20 weeks after nephrectomy were Msx2; carbonic anhydrases III, IV, VIII, IX, and XIII; MGP; osteoprotegerin; PTH receptor-1; annexins II and V; and CD39. Despite the absence of expression changes in the previous genes, many other genes were overexpressed at week 20, as shown in Fig. 3, thereby reflecting the classical complexity traditionally described for VC. This complexity forced us to analyze the gene expression changes at earlier times, which led us to organize the pattern of changes as follows: late overexpressing genes that needed 20 weeks to be noticed were osteopontin, the ectonucleotide pyrophosphatase/phosphodiesterase 1 (ENPP1), carbonic anhydrase II, and the homeobox gene A10, HOXA10 (Fig. 3A). Earlier genes, overexpressed at week 16, included the osteoblast differentiation transcription factor Runx2, TNFα, Phospho1, and the phosphate transporters PiT1 and PiT2. Genes that were overexpressed at week 12 (i.e., coinciding with significantly increased calcium), included Bmp2, the PPi transport regulator ANKH, and the antiaging protein Klotho. And finally, two genes were found to be overexpressed **before** the calcium increase in the aorta (i.e., at week 11): TNAP and the Wnt signaling pathway inhibitor Dkk1. Curiously, both RNA expressions changed similarly, with a small but significant

increase at week 11, followed by a sharp overshoot at week 12, and a progressive reduction of expression that was nevertheless still significant at weeks 16 and 20.

Histochemical analysis: To check that the RNA overexpression was causing a subsequent protein increase, TNAP, BMP2, and Klotho protein expressions were studied by IHC (Fig. 4). The three proteins had clearly increased at the time of RNA overexpression. TNAP was expressed evenly in the media and at the limit with the adventitia. BMP2 and Klotho were more abundant in the outer region of the media. In the case of Klotho, two antibodies were used successfully with similar results: one antibody from Santa Cruz Biotechnology, which recognizes an internal region of Klotho, and a second antibody that recognizes the KL2 region. The antibody KM2076 (KO603) against the KL1 region did not work for us.

In the case of TNAP, activity was also studied in the aortas, in addition to the RNA and protein abundance. Activity was determined using the chromogenic substrates BCIP/NBT and fast blue RR salt (Fig. 5A). The results showed that the maximal activity was present in the same structures of TNAP expression in the aorta, i.e., in areas of the media close to the adventitia. Activity was increased at all times in the NX animals compared to the control animals, but the intensity was higher as from week 12 of nephrectomy. Interestingly, staining of adjacent slices with alizarin red revealed that TNAP was not expressed in the areas of massive calcification, which were only present at week 20. Instead, TNAP was mainly expressed in areas without gross calcification, as in the previous weeks as from nephrectomy.

Because one of the roles of TNAP is the hydrolysis of the calcification inhibitor pyrophosphate, we quantified the PPi content in the aortas. The results, summarized in Fig. 5B, show the absence of differences in PPi content, which coincides with the absence of a PPi concentration in the plasma.

Ultrastructural analysis of TNAP expression: For a more detailed study of the localization of TNAP and of the relationship with the calcification areas, we located the TNAP protein in the aortas at 11 and 12 weeks as from nephrectomy by FSEM analysis using gold-tagged

secondary antibodies (Fig. 6). No calcifications were observed at 11 weeks, and TNAP was expressed in delimited areas such as the smooth muscle cells or elastin fibers. After 12 weeks, we observed that the calcium deposits were accompanied by TNAP expression, with no exception. Energy emission spectra revealed, among other atoms, the presence of gold with or without calcium (12 weeks and 11 weeks, respectively) (Fig. 6).

Discussion

Despite the high prevalence of VC in CKD, the life-threatening morbidity in hemodialysis patients, and the intense research over the last fifteen years, our understanding of VC pathogenesis is far from satisfactory.[2] There are several reasons for this deficient situation. First, VC is a very complex degenerative process, with the complexity arising from the involvement of multiple organs, agents, and signals. Only recently have we begun to understand this kind of systems pathology, exemplified by the relevance of the mineral and bone disorder in the nosology of VC.[1] Second, when calcification becomes visually apparent, the distorted artery wall is already a chaotic battlefield of molecules that have unclear roles in the calcification process and that are extremely difficult to untangle.[15] Third, with the logical objective of simplifying this complexity, the scientific community has been using *in vitro* methods of calcification that, unfortunately, were unrelated to cell-mediated ectopic calcification.[14]

In this work, our purpose has been to disentangle the complexity of VC by using an experimental approach that has sufficient clarity: we have focused on the very early pathogenic steps, while assuming that the complexity of advanced calcification is a consequence of an increasing and self-complicating morbid process. We chose the evolution of artery calcium content as from nephrectomy as the baseline for a time-course study of pathogenic events until a frank calcification was observed. In order to simplify the experimentation, we used two main groups of animals: control, sham-operated rats fed with a 0.6% Pi diet, and 5/6NX animals fed with a 1.2% Pi diet. We did not use 5/6NX rats fed with a 0.6% Pi as a main group, because a high intake of Pi mainly accelerates CKD and the course of VC, similar to vitamin D_3 supplementation.[13,16,17]

According to these experimental conditions, we have observed increases in aortic calcium after 12 weeks of CKD, caused by the deposition of calcium phosphate microparticles in scattered areas of the artery wall (Fig. 2D and 6). It should be noted that these incipient microdeposits were not detected visually using either alizarin red or von Kossa stains. Recently, a paper by

Professor Moe's group[18] has shown that aortic VSMC from CKD rats exhibit a reduction in the concentration of intracellular resting calcium during early calcification, which is followed by an increased concentration in advanced calcification. Both findings are compatible, because the microprecipitates that we have observed should be washed away during the isolation process of SMC, therefore making it impossible to quantify this calcium from microdeposits.

After having found the first deposits, we looked for other players in the process, before and after week 12. The expressions of 27 genes were analyzed by real-time PCR, and 15 of them were overexpressed in an orderly fashion. Space limitations prevent us from interpreting all the changes we have observed, wherefore we have limited this discussion to the most relevant changes. The expressions of TNAP and Dkk1, for example, increased one week before the calcium content did, with a maximal peak at week 12, subsequently followed by an abrupt reduction. This reduction could explain why the activity of TNAP was not observed in areas of maximal (advanced) calcification (Fig. 5). Even though the precise functions of TNAP are not known,[19] the relationship between TNAP and VC has been clearly demonstrated in several studies, and it has been associated with the hydrolysis of the calcification inhibitor, PPi. For example, TNAP overexpression in aortas has been described in adenine-fed uremic rats, and while calcification was prevented through a control diet containing 0.95% calcium and 0.4% phosphorus, the aortas exhibited increased PPi hydrolysis activity.[20] Similar overexpression has been described in patients in hemodialysis.[21] Notably, calcifications in both the media and intima of arteries have been induced in mice with normal renal function, but they had also, respectively, overexpressed TNAP in both the media[4] and intima[21] of arteries. It has been proposed that TNAP is loaded into calcifying extracellular vesicles to control the ratio of PPi/Pi[22] and that this process is mediated by the trafficking role of sortilin.[23] Similarly to previous studies,[4,20] and despite the increased TNAP expression and activity, we did not observe changes in the PPi concentration in blood plasma or aorta tissue (Table 1). TNAP activity in the plasma is inhibited by the high concentration of Pi, but this cannot explain the absence of an

effect in the aorta. One possibility is that the changes in PPi concentration are limited to very specific areas that can help the nidus formation for precipitation. This is a feasible explanation, because only a scattering of precipitates were observed. Moreover, once precipitation has started in a nidus, the deposit will grow continuously, thermodynamically favored, as we have previously reported.[14,24,25] The growth of deposits follows the classical pattern of crystallization, also described in our previous works: deposits are first formed by amorphous calcium phosphates, which will irreversibly evolve into hydroxyapatite (Fig. 2B). It is important to stress that TNAP should promote VC, but it will hardly initiate calcification. This is because homogeneous precipitation cannot take place,[14] and heterogeneous precipitation needs, in addition to PPi depletion, the presence of specific nidi, for example provided by degraded elastin,[26] extracellular vesicles, or apoptotic bodies.[27] As we have described, TNAP overexpression during CKD is limited to specific areas of the media, while transgenic overexpression in the media[4] and intima[21] affects all the cells of these structures, most likely causing extraordinary effects.

Several factors could cause TNAP overexpression in the aorta wall, although the classical upregulator, TNFα, should be excluded, because this cytokine is only increased after 16 weeks (Fig. 3). However, Wnt pathway agents involved in renal repair are also altered before the calcium increase and could participate in TNAP overexpression. In the aorta, Dickkopf-1 (Dkk1), is increased at week 11 or earlier, and it is an inhibitor (negative feedback) of the Wnt pathway involved in renal injury repair.[1] Dkk1 is released into the plasma to act in extrarenal tissues, and the antibody-mediated Dkk1 neutralization results in improved vascular function and a decrease of both osteoblastic transition and vascular calcification.[11] Table 1 shows that circulating Dkk1 was not modified up to week 20, but the expression of Dkk1 increased in the aorta wall after 11 weeks (Fig. 3). Curiously, the transduction-mediated expression of Dkk1 in endothelial cells induces a mineralizing myofibroblast phenotype, in addition to osteogenic markers, SM22, type I collagen, osterix, Runx2, and alkaline phosphatase.[12] Therefore, Dkk1 could be involved in the

TNAP overexpression that we have observed concomitant with Dkk1 upregulation. In turn, Dkk1 could be upregulated by another renal repair factor that is also released into circulation by an injured kidney, i.e., activin-A.[13] We have observed an increased plasma concentration of activin A as from the first measurement (week 11), and while in our CKD-model we did not observe changes in circulating Dkk1, it is tempting to conclude that circulating activin A could be involved in Dkk1 aortic overexpression and that this Wnt inhibitor could, in turn, increase TNAP expression and activity.

Coinciding with the calcium increase in the aorta, Bmp2, ANKH, and Klotho were upregulated at week 12 (Fig. 3). The expression of Klotho in aortas has been a permanent matter of debate,[17,28-30] but we have determined the expression of Klotho RNA and protein, in this case using two different antibodies (Fig. 4). The Pi transporters PiT1 and PiT2 were upregulated 16 weeks after nephrectomy, before hyperphosphatemia and hyperparathyroidism were determined. The role of these transporters and Pi transport in hyperphosphatemia and VC has also been debated,[31,32] but here we are reporting that the Pi transporter expression increase occurs at a late stage of VC pathogenesis and before hyperphosphatemia is detected, and therefore the precise role of these transporters in VC remains unclear.

Finally, it is interesting to note that we have not observed inhibition of the expression of VC inhibitors such as MGP or OPG (or PPi). Therefore, it is tempting to conclude that, even though VC inhibitors are very efficacious in the prevention of ectopic calcification during homeostatic conditions, they become insufficient when procalcific signals produced by an injured kidney in uremia favor the deposition of calcium phosphates in existing nidi.

In summary, in this work we have tried to clarify the order of the high number of events that participate in VC pathogenesis. While FGF23 and activin A increase rapidly in uremic plasma, as previously described,[13,33] calcium deposition in the aorta is only preceded by TNAP and Dkk1, among the agents that we have studied. Genes that are up-regulated after calcium deposition and that could therefore have a secondary role in VC include Runx2, Pi transporters,

TNFα, Phospho1, OPN, and most likely Bmp2 and Klotho. More studies are necessary to expand the list of additional agents and define the specific roles according to the order of expression during the pathogenesis of VC.

Methods

Animal experimentation. 5/6-nephrectomized (5/6NX) male Wistar rats were obtained from Janvier Labs (Saint Berthevin Cedex, France). After a week of adaptation (0 weeks in Fig. 1), they were fed *ad libitum* either 1.2% or 0.6% Pi-containing fodder (Provimi Kliba SA, Penthalaz, Switzerland) with free access to water. The animals were cared for in accordance with the EU Directive 2010/63/EU for animal experiments, and all procedures were approved by the Ethical Committee of the University of Zaragoza (ref. PI39/15). The animals were sacrificed by exsanguination.[34] Aortas were peeled off, sectioned in 4-mm segments, and used as described below.

Biochemical and enzyme-linked immunosorbent (ELISA) assays. Plasma Ca^{2+}, Pi, creatinine, urea and PPi were determined using colorimetric kits. Blood plasma FGF23, the parathyroid hormone (PTH), soluble Klotho, DKK1 and Activin A were quantified using ELISA kits.

Real-Time PCR. Total RNA from the aorta segments was retrotranscribed using a PrimeScript RT Master Mix kit, and amplification was performed using a SYBR Premix Ex Taq II kit (both from Takara Clontech, Mountain View, CA) on a LightCycler 1.5 (Roche Applied Science, Mannheim, Germany). The sequences of the primers used are presented in table S1.

Optical microscopy. Aorta segments were fixed with 4% paraformaldehyde in PBS, sucrose-cryoprotected, and embedded in optimal cutting temperature (OCT) compound.[34] Five-micrometer sections were obtained with a cryostat (Leica, Wetzlar, Germany). For immunohistochemistry, a Vectastain Elite ABC kit was used with an ImmPACT DAB Peroxidase substrate (Vector Laboratories, Burlingame, CA). TNAP and Bmp2, and Klotho antibodies used are listed in table S2. The alkaline phosphatase activity of tissue sections was determined using the chromogenic substratesBCIP/NBT and fast blue RR. For the study of aortic calcification by light microscopy, the rings were stained with alizarin red and von Kossa dyes for calcium and phosphate, respectively.[24,34]

Electron microscopy. For the ultrastructural and chemical analysis of deposits, a field emission scanning electron microscope (FESEM) from Carl Zeiss MERLIN equipped with an energy-dispersive spectroscopy (EDS) system (INCA 350, Oxford Instruments) was used on aortic rings.[24] TNAP was immunodecorated with a 10-nm gold particles-conjugated antibody.

Statistics. The data were analyzed using GraphPad Prism 5. The Gaussian distribution of data was analyzed using a Brown-Forsythe test. In normal distributions, the significances of differences were determined by a one-way ANOVA and a Tukey posttest, or a t-test. The Kruskal-Wallis and the Mann-Whitney tests were used in the absence of a normal distribution.

Disclosure

Nothing to disclose.

References

1. Seifert ME, Hruska KA. The Kidney-Vascular-Bone Axis in the Chronic Kidney Disease-Mineral Bone Disorder. *Transplantation*. 2016;100:497-505.
2. Lanzer P, Boehm M, Sorribas V et al. Medial vascular calcification revisited: review and perspectives. *Eur Heart J.* 2014;35:1515-1525.
3. Shanahan CM, Cary NR, Salisbury JR et al. Medial localization of mineralization-regulating proteins in association with Mönckeberg's sclerosis: Evidence for smooth muscle cell mediated vascular calcification. *Circulation.* 1999;100: 2168–2176.
4. Sheen CR, Kuss P, Narisawa S et al. Pathophysiological role of vascular smooth muscle alkaline phosphatase in medial artery calcification. *J Bone Miner Res*. 2015;30:824-836.
5. Kiffer-Moreira T, Yadav MC, Zhu D et al. Pharmacological inhibition of PHOSPHO1 suppresses vascular smooth muscle cell calcification. J Bone Miner Res. 2013;28:81-91.
6. Reynolds JL, Skepper JN, McNair R et al. Multifunctional roles for serum protein fetuin-a in inhibition of human vascular smooth muscle cell calcification. *J Am Soc Nephrol.* 2005;16:2920–2930.
7. Kapustin AN, Chatrou ML, Drozdov I et al. Vascular smooth muscle cell calcification is mediated by regulated exosome secretion. *Circ Res*. 2015;116:1312-1323.
8. Mizobuchi M, Ogata H, Hatamura I et al. Up-regulation of Cbfa1 and Pit-1 in calcified artery of uraemic rats with severe hyperphosphataemia and secondary hyperparathyroidism. *Nephrol Dial Transplant.* 2006;21:911-916.
9. Pai A, Leaf EM, El-Abbadi M et al. Elastin degradation and vascular smooth muscle cell phenotype change precede cell loss and arterial medial calcification in a uremic mouse model of chronic kidney disease. *Am J Pathol*. 2011;178:764-773.
10. Hu MC, Shiizaki K, Kuro-o M et al. Fibroblast growth factor 23 and Klotho: physiology and pathophysiology of an endocrine network of mineral metabolism. *Annu Rev Physiol.* 2013;75:503-33.

11. Fang Y, Ginsberg C, Seifert M et al. CKD-induced wingless/integration1 inhibitors and phosphorus cause the CKD-mineral and bone disorder. *J Am Soc Nephrol.* 2014;25:1760-1773.
12. Cheng SL, Shao JS, Behrmann A et al. Dkk1 and MSX2-Wnt7b signaling reciprocally regulate the endothelial-mesenchymal transition in aortic endothelial cells. *Arterioscler Thromb Vasc Biol*. 2013;33:1679-1689.
13. Agapova OA, Fang Y, Sugatani T et al. Ligand trap for the activin type IIA receptor protects against vascular disease and renal fibrosis in mice with chronic kidney disease. *Kidney International* 2016;89:1231-1243.
14. Hortells L, Sosa C, Millán Á et al. Critical parameters of the in vitro method of vascular smooth muscle cell calcification. PLoS One. 2015;10:e0141751.
15. Rukov JL, Gravesen E, Mace ML et al. Effect of chronic uremia on the transcriptional profile of the calcified aorta analyzed by RNA sequencing. *Am J Physiol Renal Physiol*. 2016;310:F477-F491.
16. Shobeiri N, Adams MA, Holden RM. Vascular calcification in animal models of CKD: A review. *Am J Nephrol*. 2010;31:471-481.
17. El-Abbadi MM, Pai AS, Leaf EM et al. Phosphate feeding induces arterial medial calcification in uremic mice: role of serum phosphorus, fibroblast growth factor-23, and osteopontin. *Kidney Int*. 2009;75:1297-1307.
18. Moe SM, Duan D, Doehle BP et al. Uremia induces the osteoblast differentiation factor Cbfa1 in human blood vessels. *Kidney Int.* 2003;63:1003–1011.
19. Buchet R, Millán JL, Magne D. Multisystemic functions of alkaline phosphatases. *Methods Mol Biol*. 2013;1053:27-51.
20. Lomashvili KA, Garg P, Narisawa S, et al. Upregulation of alkaline phosphatase and pyrophosphate hydrolysis: potential mechanism for uremic vascular calcification. *Kidney Int*. 2008;73:1024–1030.

21. Savinov AY, Salehi M, Yadav MC et al. Transgenic Overexpression of Tissue-Nonspecific Alkaline Phosphatase (TNAP) in Vascular Endothelium Results in Generalized Arterial Calcification. *J Am Heart Assoc.* 2015;4. pii: e002499.

22. Anderson HC, Sipe JB, Hessle L et al. Impaired calcification around matrix vesicles of growth plate and bone in alkaline phosphatase-deficient mice. *Am J Pathol*. 2004;164:841-847.

23. Goettsch C, Hutcheson JD, Aikawa M et al. Sortilin mediates vascular calcification via its recruitment into extracellular vesicles. *J Clin Invest*. 2016;126:1323-1336.

24. Martín-Pardillos A, Sosa C, Millán Á et al. Effect of water fluoridation on the development of medial vascular calcification in uremic rats. *Toxicology*. 2014;318:40-50.

25. Villa-Bellosta R, Millan A, Sorribas V. Role of calcium-phosphate deposition in vascular smooth muscle cell calcification. *Am J Physiol Cell Physiol*. 2011;300:C210-C220.

26. Pai A1, Leaf EM, El-Abbadi M et al. Elastin degradation and vascular smooth muscle cell phenotype change precede cell loss and arterial medial calcification in a uremic mouse model of chronic kidney disease. *Am J Pathol.* 2011;178:764-773.

27. Reynolds JL, Joannides AJ, Skepper JN et al. Human vascular smooth muscle cells undergo vesicle-mediated calcification in response to changes in extracellular calcium and phosphate concentrations: a potential mechanism for accelerated vascular calcification in ESRD. *J Am Soc Nephrol.* 2004;15:2857-2867.

28. Mencke R, Harms G, Mirković K, et al.; NIGRAM Consortium. Membrane-bound Klotho is not expressed endogenously in healthy or uraemic human vascular tissue. *Cardiovasc Res*. 2015;108:220-231.

29. Chang JR, Guo J, Wang Y et al. Intermedin1-53 attenuates vascular calcification in rats with chronic kidney disease by upregulation of α-Klotho. *Kidney Int*. 2016;89:586-600.

30. Lim K, Lu TS, Molostvov G et al. Vascular Klotho deficiency potentiates the development of human artery calcification and mediates resistance to fibroblast growth factor 23. *Circulation*. 2012;125:2243-2255.

31. Giachelli CM. The emerging role of phosphate in vascular calcification. *Kidney Int*. 2009;75:890-897.

32. Villa-Bellosta R, Bogaert YE, Levi M et al. Characterization of phosphate transport in rat vascular smooth muscle cells: implications for vascular calcification. *Arterioscler Thromb Vasc Biol*. 2007;27:1030-1036.

33. Christov M, Waikar SS, Pereira RC, Havasi A, Leaf DE, Goltzman D, Pajevic PD, Wolf M, Jüppner H. Plasma FGF23 levels increase rapidly after acute kidney injury. *Kidney Int*. 2013;84:776-785.

34. Martín-Pardillos A, Sosa C, Sorribas V. Arsenic increases Pi-mediated vascular calcification and induces premature senescence in vascular smooth muscle cells. *Toxicol Sci*. 2013;131:641-653.

Acknowledgments

None

Table 1. Blood plasma parameters in control and uremic rats after the indicated weeks of nephrectomy.

Parameter	Control	11 weeks	12 weeks	16 weeks	20 weeks	p ANOVA
Urea mg/dL	41.0±1.3	57.1±0.9*	59.3±5.5*	66.0±8.5*	77.3±10.0*	0.0003
Creatinine mg/dL	0.21±0.02	0.46±0.10*	0.58±0.06*	0.63±0.09*	0.76±0.10*#	<0.0001
Ca^{2+} mg/dL	1.89±0.02	2.05±0.07	1.89±0.04	1.78±0.12	1.81±0.03	0.0589
Pi mg/dL	11.9±0.4	14.0±0.5	13.7±1.1	14.5±1.1	33.4±5.7*#	<0.0001
FGF23 ng/mL	0.11±0.05	1.48±0.26	2.50±0.58*	2.76±0.74*	5.04±1.17*#	<0.0001
PTH pg/mL	0.88±0.20	0.50±0.04	0.40±0.06	0.98±0.26	17.0±3.6*#	<0.0001
TNFα ng/mL	7.22±0.09	7.18±0.08	7.09±0.10	7.33±0.13	7.45±0.18	0.4465
PPi mmol/L	6.58±0.74	11.3±2.66	11.5±0.48	6.83±1.77	6.22±1.37	0.0323
Klotho ng/mL	0.36±0.05	0.61±0.10	0.35±0.04	0.46±0.81	0.42±0.05	0.6958
Activin A pg/mL	6.04±0.82	26.2±8.5*	33.6±7.3*	32.2±5.8*	22.8±2.0*	<0.0001
Dkk1 pg/mL	73.9±18.2	62.4±9.6	76.2±8.6	92.3±22.3	80.7±11.2	0.9553

*Statistically different from control values. #Statistically different from the 11th week value. Control data are the pool of all control animals form the 4 time points because they were similar and statistically non-different. The rest of values are the mean±sem of 5 animals.

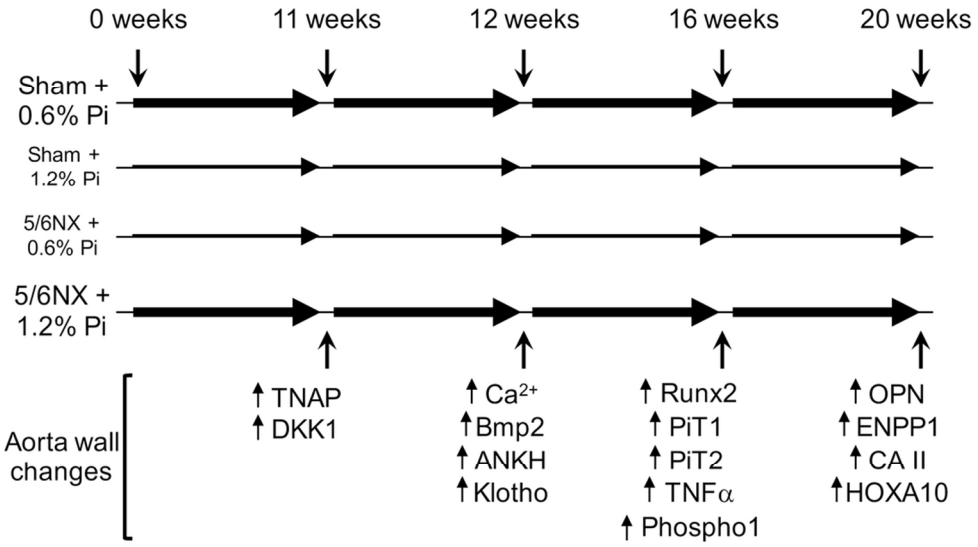

Figure 1. Diagram of the experimental design, with the time points of assay and the main findings in the aorta wall. In addition to the two experimental groups, some confirmatory experiments included four groups, namely control and 5/6NX animals with 0.6% and 1.2% Pi diets.

49x27mm (600 x 600 DPI)

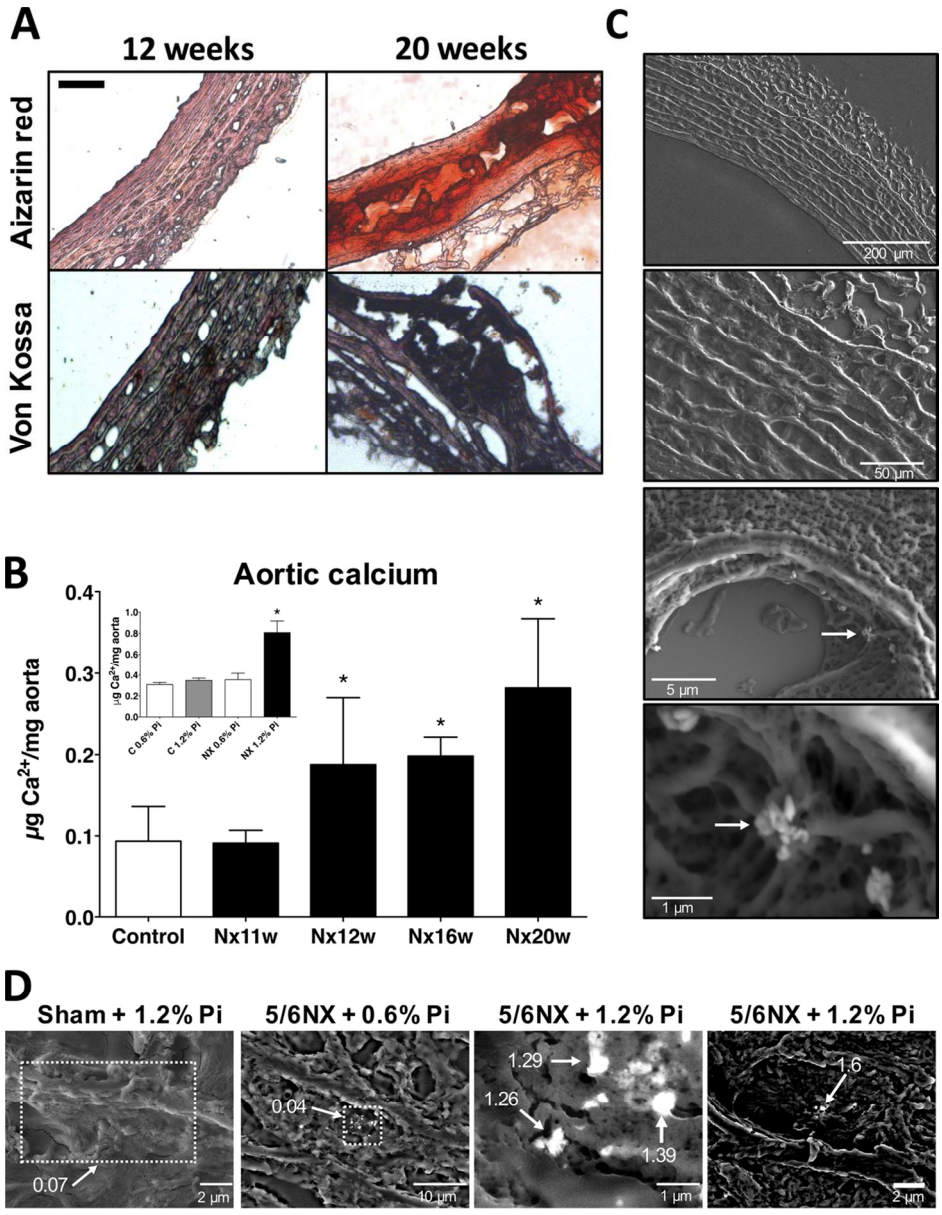

Figure 2. Time course of aorta calcification. A. Alizarin red and von Kossa staining of aorta sections at the indicated times of nephrectomy. Bar, 50 μm. B. Colorimetric quantification of aortic calcium at the indicated times. Inset, calcium content at 12 weeks in control and nephrectomized animals fed with 0.6% and 1.2% Pi food. *Significantly different ($p < 0.05$; ANOVA) from control. C. Topographic images of SEM showing calcium deposits in 12-week aortas of nephrectomized animals fed with a 1.2% Pi diet. Arrow, calcium deposits. D. Representative chemical images of aortas showing the Ca/P ratios of deposits, which can only be observed after 12 weeks in nephrectomized animals fed with a 1.2% Pi diet. In the absence of apparent deposits, an atomic analysis of the delimited areas in sham-operated rats fed with a 1.2% Pi diet or nephrectomized animals fed with a 0.6% Pi diet for 12 weeks revealed no significant calcium or phosphate content.

111x143mm (300 x 300 DPI)

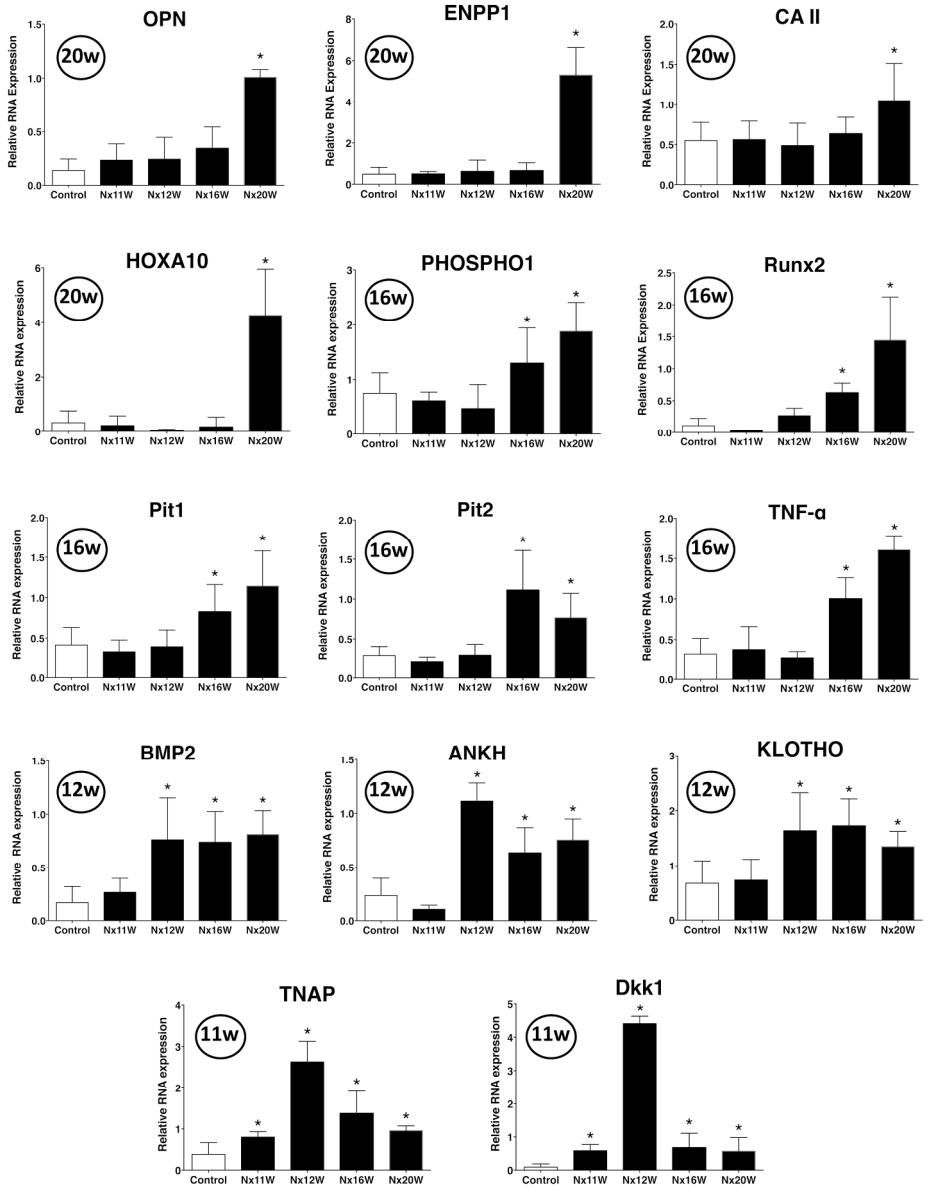

Figure 3. RNA expression of selected agents related to calcification as a function of weeks as from nephrectomy. Weeks of the first increase are shown in circles. TNAP and Dkk1 were the first genes overexpressed, even before calcium increased in the aorta wall. Asterisks indicate significant differences with respect to the pool of controls at every time week. *Significantly different ($p < 0.05$) from control. TNAP, Dkk1, Bmp2, ANKH, Klotho, TNFα, OPN, ENPP1 and CA II were analyzed with ANOVA; Phospho1, Runx2, PiT1, PiT2 and HOXA10 were analyzed with Kruskal-Wallis test.

109x137mm (600 x 600 DPI)

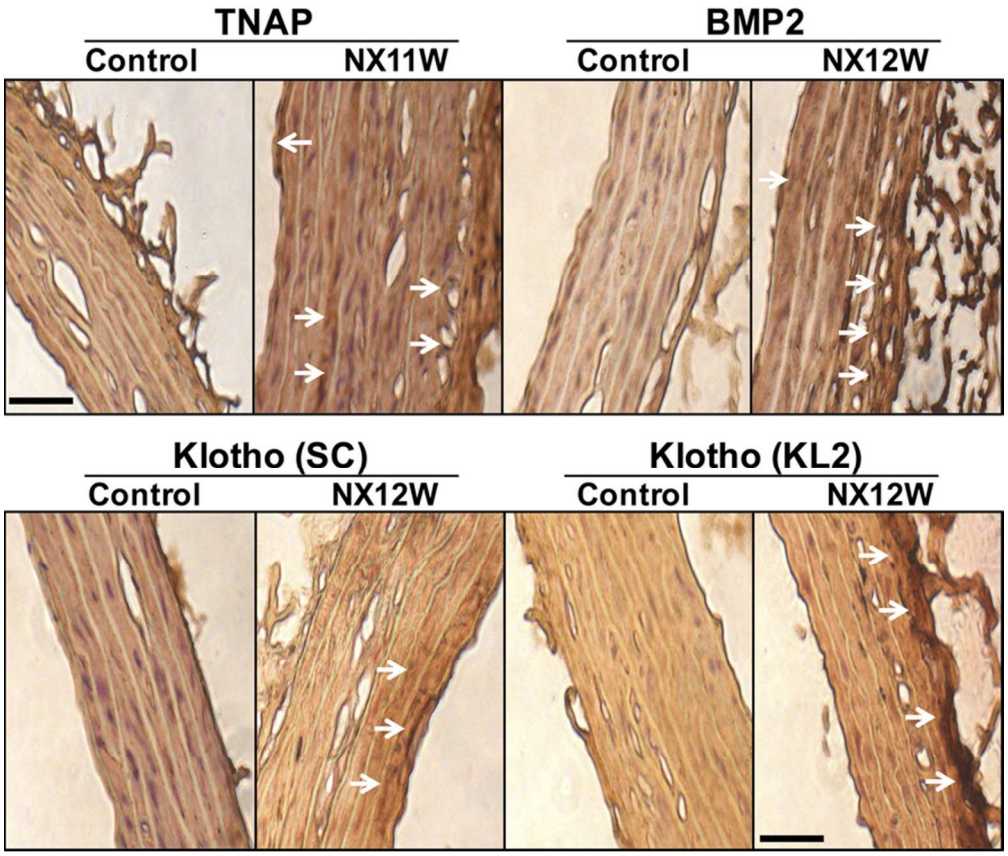

Figure 4. Immunohistochemistry of the indicated antigens and at weeks as from nephrectomy in rat arterial wall. Arrows, examples of expressed antigens. Klotho expression is shown with two different antibodies, either against an internal region (Santa Cruz Biotechnology) or against the Kl2 region. Bar, 50 μm.

75x64mm (300 x 300 DPI)

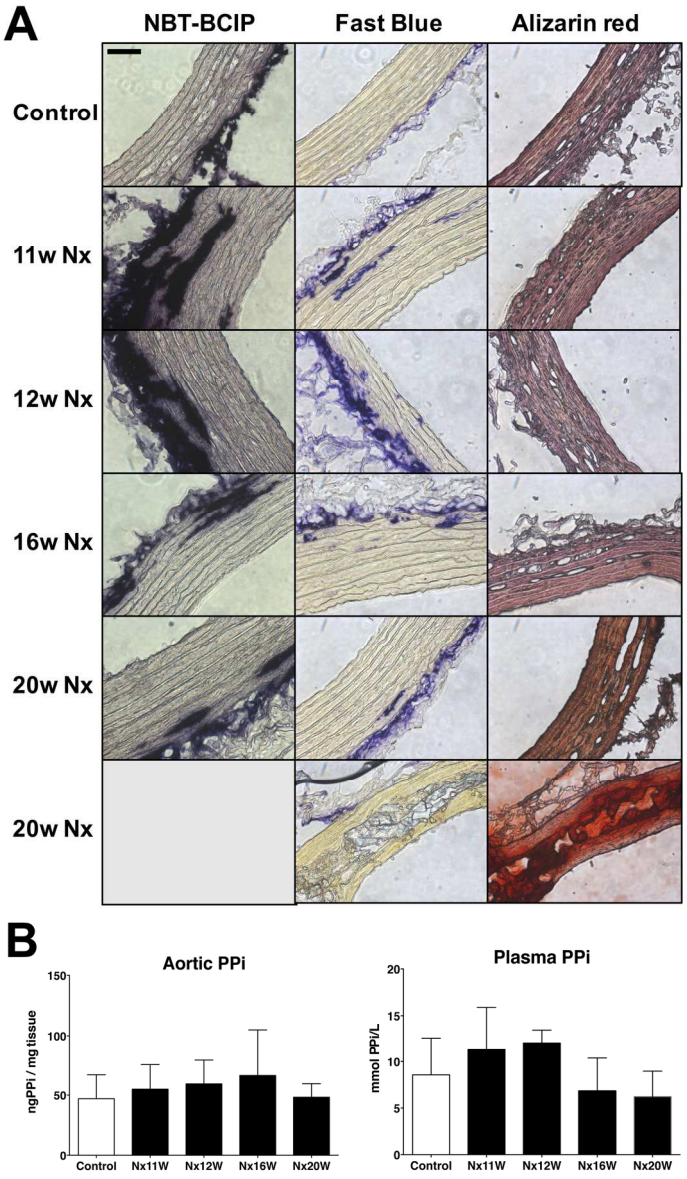

Figure 5. TNAP activity in the aortic wall. A. Staining with the chromogenic substrates of TNAP, NBT/BCIP and Fast Blue. In this case, a serial section was also stained with alizarin red to reveal calcification areas. As expected, positive staining with alizarin red was only observed in some areas at week 20, thereby revealing that gross calcification did not coincide with areas of TNAP activity. Bar, 50 µm. B. PPi content in aorta tissue at the indicated times. As a comparison, the PPi concentration in plasma is also shown. Statistical analysis with ANOVA.

141x228mm (300 x 300 DPI)

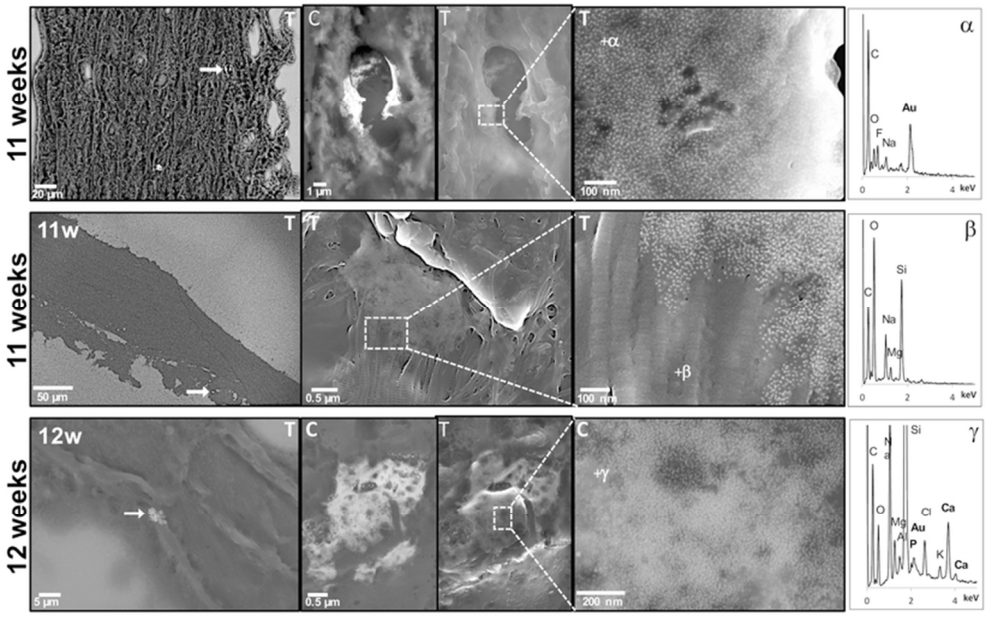

Figure 6. Ultrastructural analysis of TNAP expression and calcification by FSEM. Magnification increases to the right. Selected atomic energy spectra are shown at the right for the indicated Greek symbols. At 11 weeks as from nephrectomy, only immunogold-tagged TNAP without apparent calcification was observed in cellular areas (top) or in elastin fibers (middle). After 12 weeks, TNAP expression in incipient calcified areas was observed, as shown in the energy spectrum. C, chemical photography; T, topographic photography.

70x43mm (300 x 300 DPI)

SUPPLEMENTARY MATERIAL

Detailed Methods

Animal experimentation. Two-month old, sham-operated or 5/6-nephrectomized male Wistar rats were obtained from Janvier Labs (Saint Berthevin Cedex, France). After a week of adaptation, they were fed either 1.2% or 0.6% Pi-containing fodder with free access to food and water, in a 12 hour light cycle. In order to save animals and to simplify the experimentation, only two groups were used for the majority of the experiments: sham-operated animals fed with a 0.6% Pi diet vs. 5/6NX rats fed with a 1.2% Pi diet. For certain confirmatory and control experiments, sham-operated animals fed with a 1.2% Pi diet and 5/6NX rats fed with a 0.6% Pi diet were also used. The animals were cared in accordance with European legislation, and all procedures were approved by the Ethical Committee of the University of Zaragoza (ref. PI39/15). After anesthesia using 50 mg/kg pentobarbital i.p., samples were collected as described and the animals were sacrificed by exsanguination.[15] Aortas were peeled off, sectioned in 4-mm segments, and used as described below.

Sample preparations. The animals were anesthetized by intraperitoneal injection of pentobarbital, and samples were collected: urine was obtained with a syringe from the bladder and stored at -20º C, while blood samples were obtained from the aorta at the bifurcation of the common iliac arteries. The blood gases were analyzed immediately using Electrolytes 8 Plus cassettes in a Vetstat analyzer (both from Idexx Laboratories, Westbrook, ME), and the plasma was separated by centrifugation and stored at -20º C. The heart and complete aorta were removed, the adventitia was peeled off in ice-cold PBS, and the aortas were sectioned in 4-mm fragments and used as explained below. Some fragments were stored at -80º C for RNA extraction, while others were incubated overnight at 4º C with 0.6N HCl to quantify the calcium content of the arterial wall. Finally, the remaining fragments were processed for visual, or electron microscopy, as explained below.

Biochemical determinations. Plasma Ca^{2+}, Pi, and urea were determined colorimetrically using commercial kits from Bioassay Systems (Hayward, CA): a QuantiChrom Calcium Assay, a QuantiChrom Phosphate Assay, and a QuantiChrom Urea Assay. Plasmatic and aortic PPi was fluorometrically quantified using a High Sensitivity Pyrophosphate Assay Kit (Sigma-Aldrich, St Louis, MO). All determinations were measured in a DTX 880 Multimode plate reader (Beckman Coulter, Fullerton, CA).

Enzyme-linked immunosorbent (ELISA) assays. Blood plasma FGF23 was quantified using a Rat Fibroblast Growth Factor-23 ELISA Kit (Merck Millipore, Darmstadt, Germany) and the parathyroid hormone (PTH) using a PTH EIA Kit from Sigma-Aldrich (St Louis, MO). Soluble Klotho was quantified using a Rat Klotho ELISA Kit (CUSABIO, Wuhan, Hubei Province, China), DKK1 using an ELISA kit from Elabscience (Wuhan, China), and Activin A using an ELISA kit from RayBiotech (Norcross, GA). All determinations were measured in a DTX 880 Multimode plate reader.

Real-Time PCR. Total RNA was extracted from the aorta segments using TRIzol and was quantified using a Nanodrop (both from Thermo Scientific, Rockford, IL). The quality of the total RNA was valuated with the optical densities at 260, 280, and 320 nm and by formaldehyde gel electrophoresis. 0.5 µg total RNA was retrotranscribed using a PrimeScript RT Master Mix kit, and it was amplified using a SYBR Premix Ex Taq II kit (both from Takara Clontech, Mountain View, CA) on a LightCycler 1.5 (Roche Applied Science, Mannheim, Germany). Gene expression data were normalized to an

endogenous reference (acidic ribosomal phosphoprotein, ARP, RNA) and to a calibrator according to the manufacturer's instructions. The sequences of the primers used are presented in Online Table 1.

Microscope studies. Aorta segments were fixated with 4% paraformaldehyde (PFA) for 2 hours on ice, cryoprotected with 20% sucrose in PBS and kept at -20º C. Segments were embbeded in optimal cutting temperature (OCT) compound. 5-micrometer sections were obtained with a cryostat (Leica, Wetzlar, Germany) and were transferred onto Silane-prep slides (Sigma-Aldrich).

For immunohistochemistry studies, aortic rings were blocked for unspecific binding using 10% bovine serum albumin (BSA) and were then incubated overnight and at 4º C with the primary antibodies listed in the Online Table 2. A Vectastain Elite ABC kit was used with an ImmPACT DAB Peroxidase substrate (both from Vector Laboratories, Burlingame, CA) and biotinylated secondary antibodies, and aortic rings were observed and microphotographed with the same Axiovert 200M optical microscope (Carl Zeiss, Jena, Germany).

Aortic calcification deposits were disclosed using both light and electron microscopy. Aortic rings were stained with alizarin red and von Kossa dyes for calcium and phosphate, respectively,[1] and pictures were taken with the Axiovert 200M microscope.

For the ultrastructural analysis of deposits, a field emission scanning electron microscope (FESEM; Carl Zeiss MERLIN) equipped with an energy-dispersive spectroscopy (EDS) system (INCA 350, Oxford Instruments) was used on platinum covered aortic rings obtained from segments fixed with 2% PFA and 2.5% glutaraldehyde in PBS.[2]

Statistical analysis

The data were analyzed using GraphPad Prism 5. The Gaussian distribution of data was analyzed using a Brown-Forsythe test. In normal distributions, the significances of differences were determined by a one-way ANOVA and a Tukey posttest for multiple comparisons, or a t-test for two means. The Kruskal-Wallis test (for multiple comparation) and the Mann-Whitney test (for two means comparation) were used in the absence of a normal distribution of the sample.

References

1. Martín-Pardillos A, Sosa C, Sorribas V. Arsenic increases Pi-mediated vascular calcification and induces premature senescence in vascular smooth muscle cells. *Toxicol Sci*. 2013;131:641-653.
2. Martín-Pardillos A, Sosa C, Millán Á, Sorribas V. Effect of water fluoridation on the development of medial vascular calcification in uremic rats. *Toxicology*. 2014;318:40-50.

Table S1. Primers for real-time PCR

RNA	Sense/5'	Antisense/3'
ARP	CACCTTCCCACTGGCTGAA	TCCTCCGACTCTTCCTTTGC
TNAP	CAGAGAAAGAGAAAGACCCCAG	CTGTCACTGTGGAGACGC
Runx2	CTGCCGAGCTACGAAATGCC	GGCCACTTGGGGAGGATTTG
BMP2	GTTCTGTCCCTACTGATGAG	ATTCGGTGCTGGAAACTAC
Msx2	ACCGAAGGGCTAAGGCAAAA	CGCTGTATATGGATGCCGCT
Pit1	CCGTCAGCAACCAGATCAACTC	CCCATGCAGTCTCCCACCTTG
Pit2	CTATTCCAAGAAGAGGCTCCG	TCAGGATCGGTCAGCTCAG
PHOSP1	GCTTCCTCCTGACCTTCGAC	AGACGCGTTGCATGTACTCA
CA I	GCTGTACCCATACTCAGGAGAG	CCAGTCTGCACTTGCCATATTC
CA II	ACAGTTCCGCCTTGGTGATT	CACCACATGAGACACCTGGG
CA III	CCCTCTCTCTGGACCCTACC	TCCAGTGAACCAGGTGAAGC
CA IV	CGAACAAGGGTTCAGAGCAC	AGCACCGCAATCTTGTCCTT
CA Va	TTTCACTTCCACTGGGGAGC	CCCGTGGTGGCTTTCTTGTA
CA Vb	AGAAGCAGCCAGTTGAGGTC	ATCAGAGGTTGAAGTGGGCG
CA VI	GAGCGTGGTGTCCTTGTTCTT	GGAAGGGTACTTCTCAGGCCA
CA VII	GACAGAACGGAGTCGGCAG	GGGCGATGGGATACAGCTTG
CA VIII	GATGTCCGCCTGTCTCCAAA	GCGGTCCTCCTGACAAAACT
CA IX	CACAGGCACAGAAGTGGGAC	CGTGGTTACGTGGTTACGGA
CA X	GCCTTGTAGGTCAGTGGGAC	TCTCTTCCAGGCGGTGACTA
CA XI	CGCCATGTCTCCTTCCTACC	TTGATCTGGTGTTCGGAGCC
CA XII	TTCCCCCAGAGAAATGGTCAAC	GTGTCGGTAAGCAGTCCTTGTC
CA XIII	GACGAGCACAACGGTCCTAT	AGAGGTCGGAGTGAGGAGTC
CA XIV	GGTATGGGAATCTCGGCTGG	CCGAGCAGAGGTGAAAACCA
CA XV	AAAGTACCAGAGCATGGGGC	TTCAGACCAGACACGATGGC
MGP	AACACCTTTATATCCCCTCAGC	GCGTTGTACCCGTAGATCAG
OPG	CTCACTTGGCCTCCTGCTAA	CTTCGCACAGGGTGACATCT
OPN	CCAGCCAAGGACCAACTACA	AGTGTTTGCTGTAATGCGCC
Fetuin A	GATGACCCGGAAACAGAGCA	CCGAGACCACACCTTGACTT
ENPP1	CGAGTGGCTACAGCTTCCTAGC	TTACTGGTCCGTGTGAATGCC
PTHR1	GCATATGCGCTGGTGGATG	GTCCAGCCCTTGTCTGACTC
HOX10A	TGGTCCCTGCTCCTCTAACA	AGTATGTCATTGGGCGCGAA
ANKH	CCAACACGAACAACACGGTC	AGGCGAAGTCCACTCCAATG
OSTX	ATTGGTTAGGTGGTGGGCAG	GGGCAAAGTCAGACGGGTAA
Annexin2	CATTGCCTTCGCCTACCAGA	GGCCTAACATCACGGTCTCC
Annexin5	GTGGGGGACGGATGAAGAAA	CCCTGAGGTCTCTCGGTCAA
Klotho	TTTAGGGCGGCTCAGAAAGG	TCTCCGCCACTTCTTTGTCC

Table S2. Antibodies used in IF or IHC

Antigen	Company	Catalogue no.
ANKH	Santa Cruz Biotechnology, Inc.	sc-67242
BMP-2	Santa Cruz Biotechnology, Inc.	sc-6895
Klotho	TransGenic Inc.	KO603
Klotho	TransGenic Inc.	KO604
Phospho1	Bioss Antibodies	Abs-12562R
TNAP	Santa Cruz Biotechnology, Inc	sc-23430